The EMBO Journal Vol.18 No.22 pp.6501–6507, 1999

Major rearrangements in the 70S ribosomal 3D structure caused by a conformational switch in 16S ribosomal RNA

Irene S.Gabashvili[1,2], Rajendra K.Agrawal[1,3], Robert Grassucci[1,4], Catherine L.Squires[5], Albert E.Dahlberg[6] and Joachim Frank[1,3,4]

[1]The Wadsworth Center, [4]Howard Hughes Medical Institute, Health Research, Inc. at Wadsworth Center and [3]Department of Biomedical Sciences, State University of New York at Albany, Empire State Plaza, Albany, NY 12201-0509, [5]Department of Molecular Biology and Microbiology, Tufts University School of Medicine, Boston, MA 02111-1800 and [6]Department of Molecular and Cell Biology and Biochemistry, Division of Biology and Medicine, Brown University, Providence, RI 02912, USA

[2]Corresponding author
e-mail: irene@wadsworth.org

Dynamic changes in secondary structure of the 16S rRNA during the decoding of mRNA are visualized by three-dimensional cryo-electron microscopy of the 70S ribosome. Thermodynamically unstable base pairing of the 912–910 (CUC) nucleotides of the 16S RNA with two adjacent complementary regions at nucleotides 885–887 (GGG) and 888–890 (GAG) was stabilized in either of the two states by point mutations at positions 912 (C912G) and 885 (G885U). A wave of rearrangements can be traced arising from the switch in the three base pairs and involving functionally important regions in both subunits of the ribosome. This significantly affects the topography of the A-site tRNA-binding region on the 30S subunit and thereby explains changes in tRNA affinity for the ribosome and fidelity of decoding mRNA.

Keywords: large-scale conformational rearrangements/ mRNA channel/mRNA decoding/ribosome/rRNA switch

Introduction

The ribosome is a complex molecular machine of extraordinary precision that participates in the synthesis of polypeptides in all organisms. The rRNA plays a central catalytic role (Dahlberg, 1989; Green and Noller, 1997; Wilson and Noller, 1998) and is expected to undergo large-scale conformational rearrangements in response to small changes in secondary structure. Variations in complex multi-helix junctions connecting different regions in the 16S rRNA of the 30S subunit are very important in this respect. An example is the switch of three base pairs from positions 912–910/885–887 to 912–910/888–890 (Figure 1), which affects both the binding of tRNA to the ribosome and the decoding of the mRNA (Frattali *et al*., 1990; Lodmell *et al*., 1995; Lodmell and Dahlberg, 1997). While this switch is known to induce cooperative opening and closing of short functional helices (Lodmell and Dahlberg, 1997) surrounding the central pseudo-knot (Powers and Noller, 1991; Brink *et al*., 1993; Gutell *et al*., 1994; Vila *et al*., 1994; Samaha *et al*., 1999), the question remains as to whether any large-scale conformational changes are induced by the base pairing switch. This question can be answered by the application of three-dimensional cryo-electron microscopy (3D cryo-EM; see Frank, 1996), a method that has been used successfully in imaging the ribosome in other conformational and ligand-binding states (Agrawal *et al*., 1996, 1998, 1999a,c; Stark *et al*., 1997a,b). Here we provide evidence that large-scale structural changes do accompany the functional base pair shift in the 912/888/885 region of 16S rRNA and that they affect both ribosomal subunits. While X-ray studies of the ribosome in several laboratories are progressing toward atomic resolution of a static structure (Ban *et al*., 1998, 1999; Clemons *et al*., 1999), 3D cryo-EM makes possible the comparison of the two different 70S ribosome structures containing the two switch conformations (Lodmell and Dahlberg, 1997), and illuminates dynamic functional changes in the decoding site, providing new insights into the translational process.

Results

Large-scale rearrangements caused by the 16S RNA switch

Comparison of 3D cryo-EM maps obtained for the 70S ribosomes with alternative base pairing arrangements in the 16S RNA shows remarkable conformational differences, particularly in the 30S subunit portion (Figure 2). The head, shoulder and platform domains appear to change their relative arrangement in the ribosome, thus affecting the bridging areas to the 50S subunit, especially the central protuberance. Similar but less significant differences can also be detected between each of the mutants and wild-type ribosomes studied previously in various complexes (Malhotra *et al*., 1998; Agrawal *et al*., 1999c), suggesting a mixture of switching states for the 16S RNA in those studies.

As the mutations are exclusively in the 16S RNA (Figure 1), the 30S subunit portions of the 3D maps were isolated and analyzed in detail (Figure 3). The main differences observed between the 912–885 and 912–888 reconstructions are concentrated in the neck and body regions of the subunit. The head-to-body connection of the 30S subunit in the 912–888 conformation appears to be significantly shifted in relation to that in the 912–885 conformation, thus changing the morphology of the proposed mRNA channel (Frank *et al*., 1995a; Lata *et al*., 1996). The shoulder changes its shape and 'flattens', producing a larger space at the 30S–50S interface. The difference maps computed between the two conformations show both addition and subtraction of masses, demonstrating dramatic rearrangements in the main body, head and platform regions (Figure 3). The head appears to rotate towards the 50S subunit (shoulder-to-platform direction; Figures 3A and D, and 4A) when the

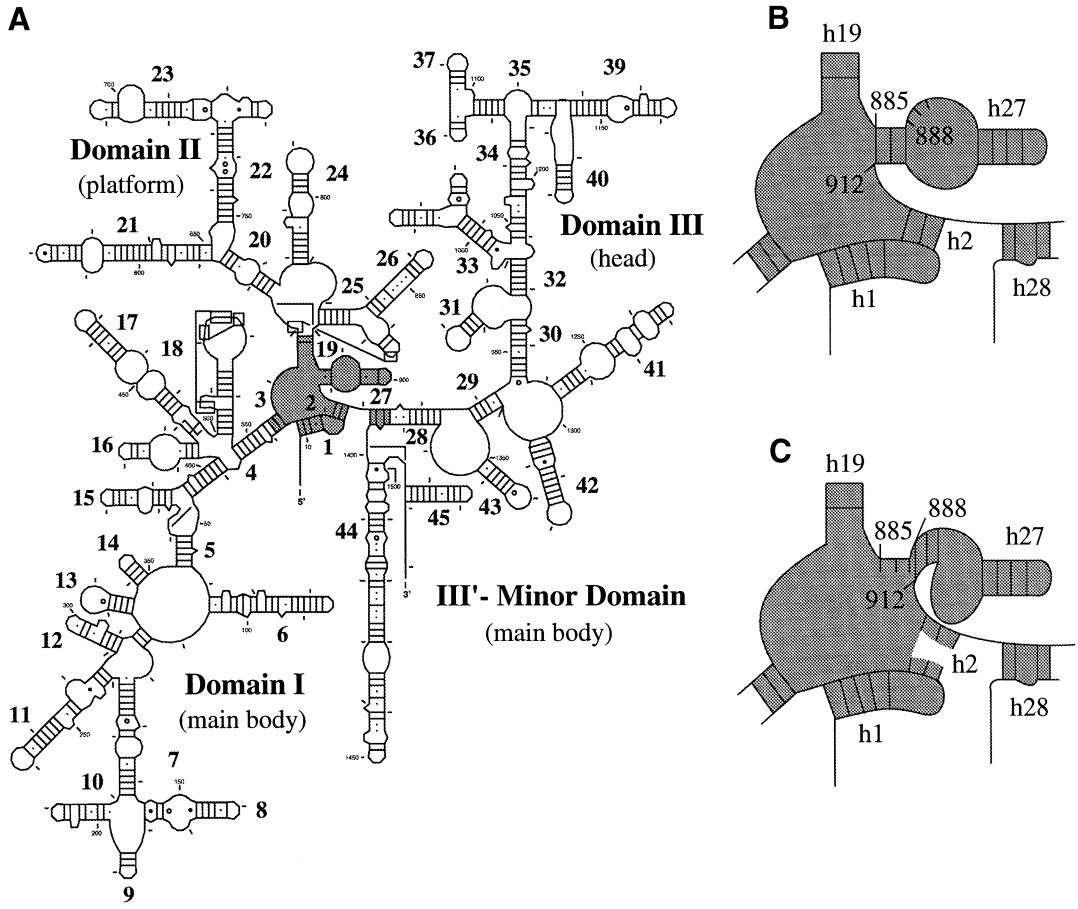

Fig. 1. (**A**) The 912 region (shaded) shown in secondary structure model of 16S RNA. Large bold numbers indicate helices according to Müller and Brimacombe (1997a), while small numbers point to RNA bases. (B and C) Schematic illustration of the 912–885 (**B**) and 912–888 (**C**) base pairing arrangements for the two 912 region conformations. Possible opening of helix 2, as proposed by Lodmell and Dahlberg (1997), is shown in (C).

16S RNA secondary structure changes from the 912–885 to the 912–888 conformation (see Figure 1). This movement is accompanied by the bending of the platform towards the L1 protein of the 50S subunit, as also seen from the appearance of the 'platform fingers' (Figure 3). The conformation of the main body changes in such a way that the lower part, including the 30S–50S subunit bridge region (B6, following the earlier nomenclature; Frank *et al.*, 1995b; Lata *et al.*, 1996), shifts closer to the 50S subunit, whereas the shoulder moves away from the 30S–50S interface side so that the 'shoulder finger' that was connected with the platform and the 50S subunit for the 912–885 conformation (bridge B3, Figure 3A and B) virtually disappears, merging with the main body (Figure 3D and E).

In order to exclude systematic influences contributing to differences observed between the reconstructions, the data sets used were matched in terms of defocus groups, numbers of particles and viewing directions. To exclude chance influences, statistical tests were computed for each data set (Liu and Frank, 1995; P.Penczek and J.Frank, in preparation). Figure 4B and C displays the resulting 3D significance maps for 99 and 97% confidence intervals, respectively.

rRNA helices and proteins involved in the rearrangement

The 912 region of the 16S rRNA, located between helices 2 and 27 (Figure 1), is placed near the junction point of the shoulder, platform and neck of the 30S subunit according to 3D models of the 16S rRNA (Müller and Brimacombe, 1997a) and recent rRNA placements into a 5.5 Å crystallographic map of the *Thermus thermophilus* 30S subunit (Clemons *et al.*, 1999). Helix 27 is connected to nucleotides 912–910 by a relatively long single-stranded region, recently proposed to be assembled into an E loop motif (Leontis and Westhof, 1998) in the 912–885 conformation. It had been assumed to extend further down into the lower part of the subunit body (Müller and Brimacombe, 1997a), but has now been placed perpendicular to the body plane pointing towards the shoulder in the crystallographic map (Clemons *et al.*, 1999). According to our significance map, the most significant changes occur near the proposed 912 region and in the lower part of the 30S subunit (see Figure 4B for $P < 0.01$, i.e. for a 99% confidence interval, indicating the highest degree of significance). The changes observed could be due in part to rearrangements of helix 44, which is connected to the central pseudo-knot and participates in the formation of B2, B3 and B5 bridges (Figure 3), identified in more detail in an 11.5 Å cryo-EM reconstruction of the fMet-tRNA$_f^{Met}$ ribosome complex (I.S.Gabashvili, R.K.Agrawal, C.M.T.Spahn, R.Grassucci, J.Frank and P.Penczek, in preparation) and in the *T.thermophilus* 30S subunit (Clemons *et al.*, 1999). At 19 Å resolution, h44 is seen only partially, requiring higher thresholds for more complete visualization. Proposed pathways of this helix are shown in Figure 4. The middle portion of helix 44, shifted closer

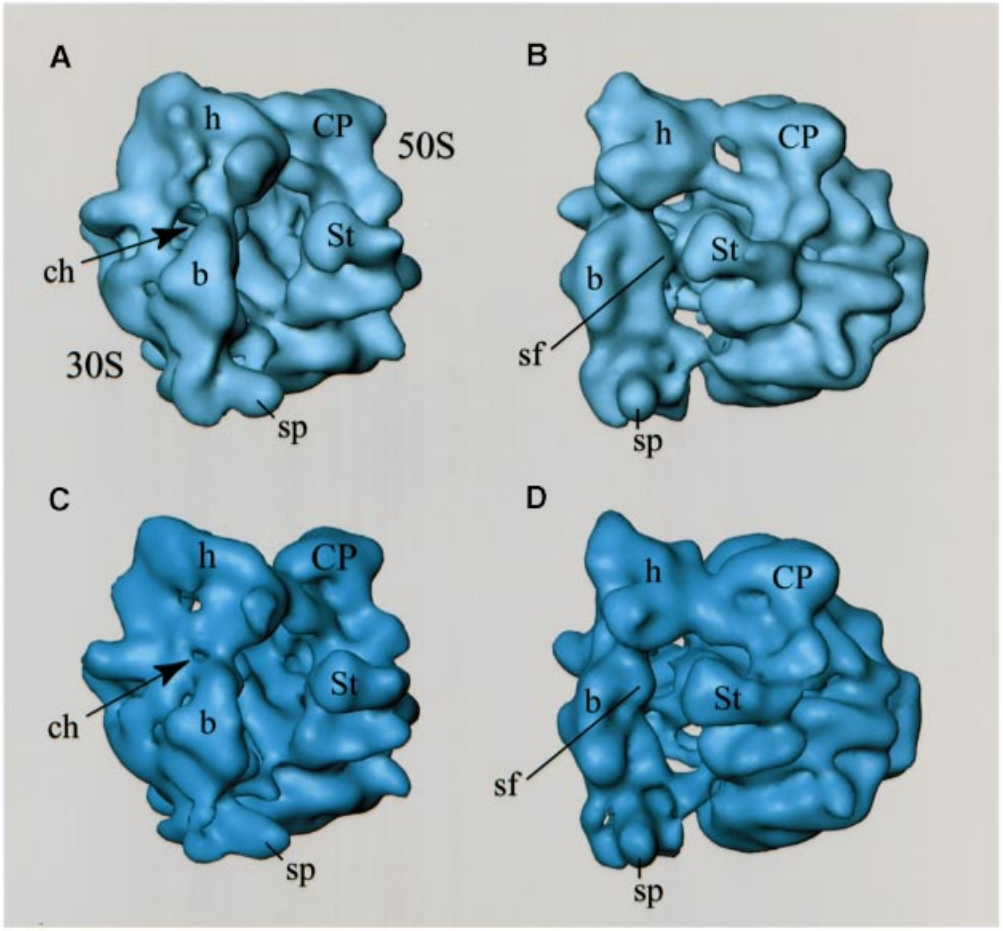

Fig. 2. The 19 Å resolution cryo-EM map of the 912–885 (**A** and **B**) and 912–888 (**C** and **D**) conformations of *E.coli* 70S ribosomes presented from different viewing angles. (A and C) 30S solvent side view showing the proposed mRNA channel; (B and D) 30S:50S side view. Those features that differ the most are: channel (ch), 'shoulder finger' (sf) region; and connection of the 30S subunit head (h) to the central protuberance area (CP) of the 50S subunit. Other features of the ribosome labeled are: b, body and sp, spur of the 30S subunit; and St, L7/L12 stalk of the 50S subunit.

to the 30S subunit body in the 912–888 conformation, participates in the formation of the intersubunit bridge B3. It is indeed important for ribosomal subunit association (Mitchell *et al*., 1992; Firpo and Dahlberg, 1998; Merryman *et al*., 1999). The changes induced by the switch may also involve protein S5, which is essential for the control of translational accuracy of the ribosome in *Escherichia coli* (Gorini, 1974; Ehrenberg *et al*., 1995), as it has been placed in the vicinity of the 30S subunit 'shoulder finger' (Müller and Brimacombe, 1997b) closer to the head-to-body connection (Clemons *et al.*, 1999). According to our difference (Figure 3) and significance maps (Figure 4) as well as crystallographic placements (Clemons *et al.*, 1999), the most significant ($P < 0.01$) changes occur in the contact area of proteins S4 and S5, possibly disrupting the interaction of these proteins.

At a slightly lower level of significance ($P < 0.02$, not shown), large perturbations in the head and the platform region can be detected. The movement of the upper 'platform finger' possibly involves dislocation of helices 22 and 23 and protein S11, known to play an essential role in the P-site tRNA selection (Rosen and Zimmermann, 1997). Rotation of the head would require transitions in other hinge regions: helix 28 and, probably, some other sites such as helix 43, the site of the other E loop motif in 16S rRNA that organizes the neighboring multi-helix structure in the head (Leontis and Westhof, 1998). Changes in the 50S subunit regions proximal to the platform, probably caused by movements of the bridging 30S subunit portions (Lata *et al*., 1996), also seem to be significant ($P < 0.03$) (Figure 4C). The regions most affected are: the central protuberance, probably involving 5S RNA (bridge B1); the mouth of the tunnel in the interface canyon; and the B3-bridging region. According to a higher resolution (11.5 Å) cryo-EM map (I.S.Gabashvili, R.K.Agrawal, C.M.T.Spahn, R.Grassucci, J.Frank and P.Penczek, in preparation) and crystallographic map of the 50S subunit (Ban *et al*., 1998, 1999), the affected bridging regions represent relatively long and isolated, and therefore potentially flexible, rRNA helices.

Discussion

Conformational difference between the mutants in the context of the available biochemical information

Localized switches such as 912/885:912/888 near the central pseudo-knot region (Figure 1) can bring about significant changes in the 16S rRNA 3D structure. Chemical probing has demonstrated that the 912 switch

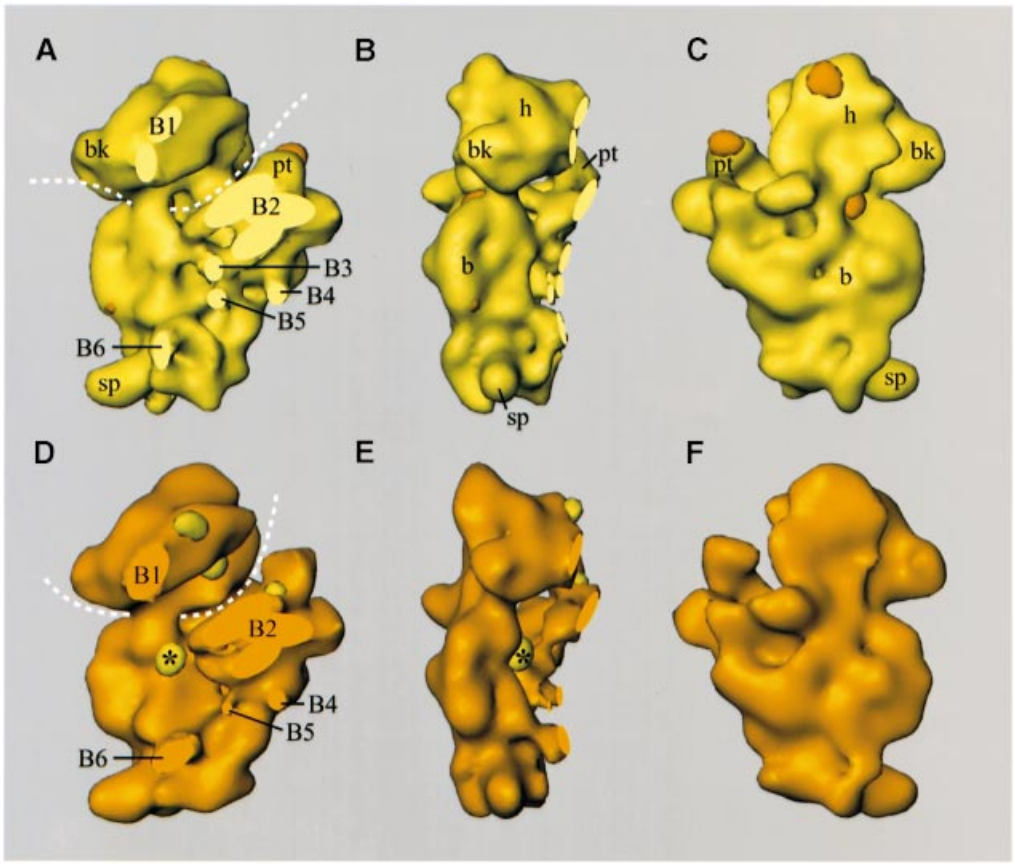

Fig. 3. 30S subunit portion of the ribosome obtained by masking off the 50S portion from 3D cryo-maps of the 70S ribosomes. The subunit is shown with the positive and negative difference maps overlaid in interface side view (**A** and **D**); in side view (**B** and **E**), as in Figure 2D and D; and in solvent side view (**C** and **F**). Top panel (yellow): the 912–885 conformation. Orange regions in (A), (B) and (C) show the mass added in the 912–885 to 912–888 transition. Bottom panel (orange): the 912–888 conformation. Yellow regions in (D), (E) and (F) show the mass added in the 912–888 to 912–885 transition. Landmarks: b, body; bk, beak; h, head; pt, platform; sp, spur; and B1–B6, 30S:50S bridges (Frank *et al*., 1995b; Lata *et al*., 1996). The white dashed lines in (A and D) represent passage of mRNA through the channel (Frank *et al*., 1999. *Marks the site where h27 of 16S RNA is proposed to be situated; the same region was found to be changed by heat activation in the 30S subunit (Lata *et al*., 1996; Agrawal *et al*., 1999b).

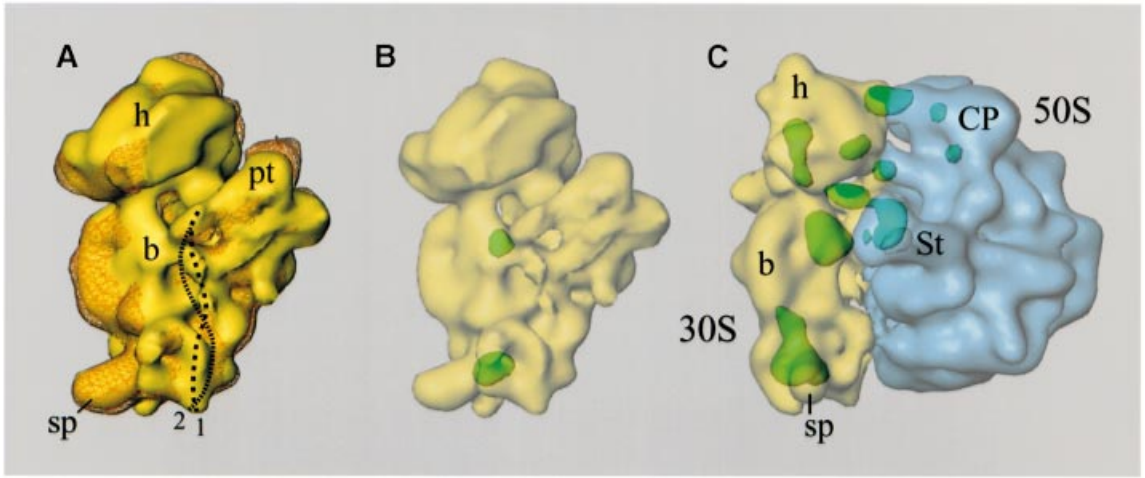

Fig. 4. (**A**) Superimposed 30S subunits of the 912–885 (yellow, solid) and 912–888 (orange, wire-mesh) conformations. Black dashed lines indicate the proposed pathway of helix 44 in the 912–885 (1) and 912–888 (2) states. (B and C) 3D cryo-EM maps of the masked 30S subunit (**B**) and the 70S ribosome (**C**), shown with 3D significance maps (green) at a $P < 0.01$ level of significance (B) at which changes are seen only in the 30S subunit, and $P < 0.03$ (C) level of significance, at which changes in the 50S subunit are also seen.

affects the conformation of helices 2, 18, 26, 28, 34, 44 and 43 (Lodmell and Dahlberg, 1997), located in potential hinge-bent regions (helices 2, 26 and 28), at the head–shoulder contact (h18 and possibly h34) and at the 30S–50S bridges (helices 26 and 44). Large-scale movements described in the present work would require changes in

these strategic regions of the 16S rRNA. It is interesting to note that the same redistributions of mass in the neck and the 'shoulder finger' regions, found here for transition from the 912–888 state (deficient in A-site binding of aminoacyl-tRNA) to the 912–885 conformation (showing strong tRNA binding), were observed previously during the heat activation of the 30S subunit (Lata *et al*., 1996; Agrawal *et al*., 1999b). The mass of density tentatively assigned to helix 2, forming the central pseudo-knot, is particularly important in this respect (see Agrawal *et al*., 1999b). It is not clear if the conformational changes induced by the heat-activated transition (Agrawal *et al*., 1999b) are related directly to conformational changes observed in the present work. However, similarities suggest that perturbations in the helix junction areas are related to functional activation of the 30S subunit (Weller and Hill, 1992), and are essential for the tRNA-binding at the A-site (Agrawal *et al*., 1996, 1998, 1999a; Stark *et al*., 1997a,b; Malhotra *et al*., 1998).

The mRNA channel and the decoding process

One of the most important regions affected by the conformational changes due to the 16S rRNA switch is the channel, located between the neck, head and shoulder of the 30S subunit. It has been proposed as the conduit for the mRNA based on cryo-EM reconstruction of 70S ribosomes (Frank *et al.*, 1995b) and isolated 30S ribosomal subunits (Lata *et al*., 1996) combined with tRNA binding (Agrawal *et al*., 1996) and mRNA cross-linking data (Dontsova *et al*., 1992; Rinke-Appel *et al.*, 1993, 1994; Sergiev *et al.*, 1997). The probable pathway of the mRNA along this route (see Müller *et al.*, 1997) was confirmed recently by direct visualization (Frank *et al*., 1999). Large rearrangements in the shoulder–head contact area, observed in the present work, could explain contradictory cross-linking results, obtained for the region presumably forming the channel-forming wall (530 loop), relative to the head (h33) and the platform (h26) (Wang *et al.*, 1999). These movements could be crucial for translation.

The 912–888 conformation has reduced tRNA binding at the A-site and an elevated rate of frameshifting. In contrast, the 912–885 conformation is able to accept even non-cognate tRNAs at the A-site and has a greater affinity for tRNA than even wild-type ribosomes. The biological effect is expressed as an increased error frequency during translation.

The hyperaccurate phenotype (912–888 conformation) is characterized by a relatively 'closed' channel and different topography at the A-site and neighboring area of the shoulder. We speculate that correct positioning of the tRNA, needed for the codon–anticodon interaction in this ribosomal conformation, is unlikely to be achieved by a diffusion-controlled process, and is energetically highly unfavorable for non-cognate tRNAs. In the 912–885 conformation, mRNA is more accessible and the topography of the site supports binding of tRNA molecules. Accordingly, the 912–885 to 912–888 transition could participate in the A-site tRNA capture and selection, initially providing an optimal conformation for binding of tRNA to both mRNA and the ribosome (referred to as initial binding in Pape *et al*., 1999) and then altering the conformation to favor dissociation of non-cognate tRNAs (912–888 state). While the channel is not actually frozen in one or the other conformation, the increased time spent by the mutant subunits in their favored form could bias maintenance of the reading frame in two different ways: (i) restricted mobility of the mRNA, trapped in the channel in the 912–888 conformation, could result in frameshifting (Atkins and Gesteland, 1999; Farabauh and Bjork, 1999), as could the empty A-site of the paused ribosome following dissociation of the non-cognate tRNA; and (ii) in the 912–885 conformation, the topography of the channel favors mRNA mobility, which could explain the higher stop codon readthrough rate (Jacobson *et al*., 1998).

While the switch appears to play a significant role in the decoding process, the mechanism by which it affects translocation is less clear. It could occur during the transition from the 912–888 to 912–885 conformation (Green and Noller, 1997; Lodmell and Dahlberg, 1997; Agrawal *et al*., 1999b), thus completing the elongation cycle with one complete switch cycle in the 912 region.

Materials and methods

Preparation of mutant ribosomes

Bacterial strain AVS 69009, a derivative of TA531, lacking all seven chromosomal *rrn* operons (Asai *et al.*, 1999), was transformed with plasmid pSTL102 (Triman *et al*., 1989), pSTL912G (restrictive phenotype, 912–888 mutant), and pSTL912G/885 U (ram phenotype, 912–885 mutant). Strains containing the plasmids were grown at 37°C in LB broth medium supplemented with ampicillin (100 μg/ml). Ribosomes were prepared as described by Stanley and Wahba (1967) with some modifications (Agrawal and Burma, 1996) and purified from the dissociated 30S and 50S particles by sucrose gradient centrifugation.

Electron microscopy

Cryo-grids were prepared as described by Wagenknecht *et al.* (1988). Micrographs were recorded on a Philips EM420 electron microscope at a magnification of 52 200× (± 2%)

Image processing

Scanning was done with a step size of 1016 d.p.i. corresponding to 4.78 Å on the object scale, on a Hi SCAN microdensitometer (model 141 by Eurocore, France).

A set of 65 micrographs was selected for both the 912–885 mutant ribosomes (with defoci ranging from 1.0 to 3.0 μ) and the 912–888 mutant (1.1–1.9 μ) after screening for the presence of Thon rings by optical diffraction. For individual reconstructions of each data set, 19 495 and 10 000 particles were used, after elimination of overrepresented views, yielding 17.1 and 19.3 Å resolution, respectively. Matching of defocus values, number of particles and viewing angles made it necessary to eliminate 9495 particles of the 912–885 data set, which reduced its resolution to 18.9 Å, closely matching the resolution of the 912–888 mutant. To prove that the large differences observed between reconstructions of the two mutant ribosomes are not caused by reconstruction artifacts, the data sets were screened repeatedly, a stronger cut-off of overrepresented views was applied and different 70S maps computed in our laboratory were taken as references for the iterative refinement procedure. However, in all cases, after angular assignments were stabilized, the final 912–888 reconstructions displayed the same differences with the conformation of the 912–885 mutant. Particles from the corresponding defocus groups of each data set were used to calculate 3D significance maps through 2D statistical variance analyses and Student's *t*-tests (Liu and Frank, 1995; P.Penczek and J.Frank, in preparation). The 30S subunit portion was extracted from the 70S volume as described earlier (Gabashvili *et al*., 1999). Final thresholds for display and comparison were chosen on the basis of volume estimations (see, for example, Verschoor *et al*., 1984).

Acknowledgements

We thank Mark Bayfield, Anton Vila and J.Stephen Lodmell for help in construction of the strains, Pawel Penczek and Christian Spahn for helpful suggestions, and Amy Heagle for assistance with the illustrations.

This work was supported by grants from the National Institutes of Health (R37 GM29169, R01 GM55440) and the National Science Foundation (BIR 9219043) to J.F. and from the National Institutes of Health (GM19756) to A.E.D. and (GM 24751) to C.L.S. Computing support was kindly provided by the National Center for Supercomputer Applications, University of Illinois at Urbana-Champaign.

References

Agrawal,R.K. and Burma,D.P. (1996) Sites of ribosomal RNAs involved in the subunit association of tight and loose couple ribosomes. *J. Biol. Chem.*, **271**, 21285–21291.

Agrawal,R.K., Penczek,P., Grassucci,R.A., Li,Y., Leith,A., Nierhaus,K.H. and Frank,J. (1996) Direct visualization of A-, P-, and E-site transfer RNAs in the *Escherichia coli* ribosome. *Science*, **271**, 1000–1002.

Agrawal,R.K., Penczek,P., Grassucci,R.A. and Frank,J. (1998) Visualization of elongation factor G on the *Escherichia coli* 70S ribosome: the mechanism of translocation. *Proc. Natl Acad. Sci. USA*, **95**, 6134–6138.

Agrawal,R.K., Heagle,A.B., Penczek,P., Grassucci,R.A. and Frank,J. (1999a) EF-G-dependent GTP hydrolysis induces translocation accompanied by large conformational changes in the 70S ribosome. *Nature Struct. Biol.*, **6**, 643–647.

Agrawal,R.K., Lata,R.K. and Frank,J. (1999b) Conformational variability in *Escherichia coli* 70S ribosome as revealed by 3D cryo-electron microscopy. *Int. J. Biochem. Cell Biol.*, **31**, 243–254

Agrawal,R.K., Penczek,P., Grassucci,R.A., Burkhardt,N., Nierhaus,K.H. and Frank,J. (1999c) Effect of buffer conditions on the position of tRNA on the 70S ribosome as visualized by cryoelectron microscopy. *J. Biol. Chem.*, **274**, 8723–8729.

Asai,T., Zaporojets,D., Squires,C. and Squires,C.L. (1998) An *Escherichia coli* strain with all chromosomal rRNA operons inactivated: complete exchange of rRNA genes between bacteria. Proc. *Natl Acad. Sci. USA*, **96**, 1971–1976.

Atkins,J.F. and Gesteland,R.F. (1999) Intricacies of ribosomal frameshifting. *Nature Struct. Biol.*, **6**, 206–207.

Ban,N., Freeborn,B., Nissen,P., Penczek,P., Grasucci,R.A., Swet,R., Frank,J., Moore,P. and Steitz,T.A. (1998) A 9-Ångstrom resolution X-ray crystallographic map of the large ribosomal subunit. *Cell*, **93**, 1105–1115.

Ban,N., Nissen,P., Hansen,J., Capel,M., Moore,P. and Steitz,T.A. (1999) Placement of protein and RNA structures into a 5 Å map of the large ribosomal subunit. *Nature*, **400**, 841–847.

Brink,M.F., Verbeet,M.P. and de Boer,H.A. (1993) Formation of the central pseudoknot in 16S rRNA is essential for initiation of translation. *EMBO J.*, **12**, 3987–3996.

Clemons,W.M., May,J.L.C., Wimberly,B.T., McCutcheon,J.P., Capel,M.S. and Ramakrishnan,V. (1999) Structure of a bacterial ribosomal subunit at 5.5 Å resolution. *Nature*, **400**, 833–840.

Dahlberg,A.E. (1989) The functional role of ribosomal RNA in protein synthesis. *Cell*, **57**, 525–529.

Dontsova,O., Dokudovskaya,S., Kopylov,A., Bogdanov,A., Rinke-Appel, J., Junke,N. and Brimacombe,R. (1992) Three widely separated positions in the 16S RNA lie in or close to the ribosomal decoding region: a site-directed cross-linking study with mRNA analogues. *EMBO J.*, **11**, 3105–3116

Ehrenberg,M., Bilgin,N., Dincbas,V., Karimi,R., Hughes,D. and Abdulkarim,F. (1995) tRNA–ribosome interactions. *Biochem. Cell Biol.*, **73**, 1049–1054.

Farabaugh,P.J. and Bjork,G.R. (1999) How translational accuracy influences reading frame maintenance. *EMBO J.*, **18**, 1427–1434.

Firpo,M.A. and Dahlberg,A.E. (1998) The importance of base pairing in the penultimate stem of *Escherichia coli* 165 rRNA for ribosomal subunit association. *Nucleic Acids Res.*, **26**, 2156–2160.

Frank,J. (1996) *Three-dimensional Electron Microscopy of Macromolecular Assemblies*. Academic Press, San Diego, CA.

Frank,J. *et al*. (1995a) A model of protein synthesis based on cryo-electron microscopy of the *E.coli* ribosome. *Nature*, **376**, 441–444.

Frank,J., Verschoor,A., Li,Y., Zhu,J., Lata,R.K., Radermacher,M., Penczek,P., Agrawal,R.K. and Srivastava,S. (1995b) A model of the translational apparatus based on three-dimensional reconstruction of the *E.coli* ribosome. *Biochem. Cell Biol.*, **73**, 757–765.

Frank,J., Penczek,P., Grassucci,R.A., Heagle,A.B., Spahn,C.M.T. and Agrawal, R.K. (1999) Cryo-electron microscopy of the translational apparatus: experimental evidence for the paths of mRNA, tRNA and the polypeptide chain. In Garrett,R.A., Douthwaite,S.R., Liljas,A., Matheson,A.T., Moore,P.B. and Noller,H.F. (eds), *The Ribosome: Structure, Function, Antibiotics and Cellular Interactions*. ASM Press, Washington, DC, in press.

Frattali,A.L., Flynn,M.K., de Stasio,E.A. and Dahlberg,A.E. (1990) Effects of mutagenesis of C912 in the streptomycin binding region of *Escherichia coli* 16S ribosomal RNA. *Biochim. Biophys. Acta*, **1050**, 27–33

Gabashvili,I.S., Agrawal,R.K., Grassucci,R. and Frank,J. (1999) Structure and structural variations of the *Escherichia coli* 30S ribosomal subunit as revealed by three-dimensional cryo-electron microscopy. *J. Mol. Biol.*, **286**, 1285–1291.

Gorini,L. (1974) Streptomycin and misreading of the genetic code. In Nomura,M., Tissiers,A. and Lengyel,P. (eds), *Ribosomes*. Cold Spring Harbor Laboratory Press, Cold Spring Harbor, NY, pp. 791–809.

Green,R. and Noller,H.F. (1997) Ribosomes and translation. *Annu. Rev. Biochem.*, **66**, 679–716.

Gutell,R.R., Larsen,N. and Woese,C.R. (1994) Lessons from an evolving rRNA: 16S and 23S rRNA structures from a comparative perspective. *Microbiol. Rev.*, **58**, 10–26

Jacobson,A.B., Arora,R., Zuker,M., Priano,C., Lin,C.H. and Mills,D.R. (1998) Structural plasticity ion RNA and its role in the regulation of protein translation in coliphage Q-beta. *J. Mol. Biol.*, **275**, 589–600.

Lata,K.R., Agrawal,R.K., Penczek,P., Grassucci,R., Zhu,J. and Frank,J. (1996) Three-dimensional reconstruction of the *Escherichia coli* 30S ribosomal subunit in ice. *J. Mol. Biol.*, **262**, 43–52.

Laughrea,M. (1994) Structural dynamics of translating ribosomes: 16S ribosomal RNA bases that may move twice during translocation. *Mol. Microbiol.*, **11**, 999–1007.

Liu,W. and Frank,J. (1995) Estimation of variance distribution in three-dimensional reconstruction. I. Theory. *J. Optic. Soc. Am. A*, **12**, 2615–2627.

Leontis,N.B. and Westhof,E. (1998) The 5S rRNA loop E-chemical probing and phylogenetic data versus crystal structure. *RNA*, **4**, 1134–1153.

Liebman,S.W., Chernoff,Y.O. and Liu,R. (1995) The accuracy center of a eukaryotic ribosome. *Biochem. Cell Biol.*. **73**, 1141–1149.

Lodmell,J.S. and Dahlberg,A.E. (1997) A conformational switch in *Escherichia coli* 16S ribosomal RNA during decoding of messenger RNA. *Science*, **277**, 1262–1267.

Lodmell,J.S., Gutell,R.R. and Dahlberg,A.E. (1995) Genetic and comparative analysis reveal an alternative secondary structure in the region of nt 912 of *Escherichia coli* 16S rRNA. *Proc. Natl Acad. Sci. USA*, **92**, 10555–10559.

Malhotra,A., Penczek,P., Agrawal,R.K., Gabashvili,I.S., Grassucci,R.A., Jünemann,R., Burkhardt,N., Nierhaus,K.H. and Frank,J. (1998) *Escherichia coli* 70S ribosome at 15-Å resolution by cryo-electron microscopy: localization of fMet-tRNA$_f^{Met}$ and fitting of L1 protein. *J. Mol. Biol.*, **280**, 103–116.

Merryman,C., Moazed,D., Daubresse,G. and Noller,H.F. (1999) Nucleotides in 16S RNA protected by the association of 30S and 50S ribosomal subunits of the *Escherichia coli* ribosome *J. Mol. Biol.*, **285**, 107–113.

Mitchell,P., Osswald,M. and Brimacombe,R. (1992) Identification of intermolecular RNA cross-links at the subunit interface of the *Escherichia coli* ribosome. *Biochemistry*, **31**, 3004–3011.

Müller,F. and Brimacombe,R. (1997a) A new model for the three-dimensional folding of *Escherichia coli* 16S ribosomal RNA. I. Fitting the RNA to a 3D electron microscopic map at 20 Å. *J. Mol. Biol.*, **271**, 524–544.

Müller,F. and Brimacombe,R. (1997b) A new model for the three-dimensional folding of *Escherichia coli* 16S ribosomal RNA. II. The RNA–protein interaction data. *J. Mol. Biol.*, **271**, 545–565.

Müller,F., Stark,H., van Heel,M., Rinke-Appel,J. and Brimacombe,R. (1997) A new model for the three-dimensional folding of *Escherichia coli* 16S ribosomal RNA. III. The topography of the functional center. *J. Mol. Biol.*, **271**, 566–587.

Pape,T., Wintermeyer,W. and Rodnina,M.V. (1999) Induced fit in initial selection and proofreading of aminoacyl-tRNA on the ribosome. *EMBO J.*, **17**, 7490–7497.

Powers,T. and Noller,H.F. (1991) A functional pseudoknot in 16S ribosomal RNA. *EMBO J.*, **10**, 2203–2214.

Rinke-Appel,J., Junke,N., Brimacombe,R., Dukudovskaya,S., Dontsova,O. and Bogdanov,A. (1993) Site-directed cross-linking of mRNA analogues to 16S ribosomal RNA; a complete scan of cross-links from all positions between '+1' and '+16' on the mRNA, downstream from the decoding site. *Nucleic Acids Res.*, **21**, 2853–2859.

Rinke-Appel,J., Junke,N., Brimacombe,R., Lavrik,I., Dokudovskaya,S., Dontsova,O. and Bogdanov,A. (1994) Contacts between 16S ribosomal RNA and mRNA, within the spacer region separating the AUG initiator codon and the Shine–Dalgarno sequence; a site-directed cross-linking study. *Nucleic Acids Res.*, **22**, 3018–3025.

Rosen,K.V. and Zimmermann,R.A. (1997) Photoaffinity labeling of 30S-subunit proteins S7 and S11 by 4-thiouridine-substituted $tRNA^{phe}$ situated at the P site of *Escherichia coli* ribosomes. *RNA*, **3**, 1028–1036.

Samaha,R.R., Joseph,S., O'Brien,B., O'Brien,T.W. and Noller,H.F. (1999) Site-directed hydroxyl radical probing of 30S ribosomal subunits by using Fe(II) tethered to an interruption in the 16S rRNA chain. *Proc. Natl Acad. Sci. USA*, **96**, 366–370.

Sergiev,P.V., Lavrik,I.N., Wlasoff,V.A., Dokudovskaya,S.S., Dontsova, O.A., Bogdanov,A.A. and Brimacombe,R. (1997) The path of mRNA through the bacterial ribosome: a site-direct crosslinking study using new photoreactive derivatives of guanosine and uridine. *RNA*, **3**, 464–475.

Stanley,W.M.,Jr and Wahba,A.J. (1967) Chromatographic purification of ribosomes. *Methods Enzymol.*, **12A**, 524–526.

Stark,H., Orlova,E.V., Rinkeappel,J., Junke,N., Müller,F., Rodnina,M., Wintermeyer,W., Brimacombe,R. and van Heel,M. (1997a) Arrangement of tRNAs in pre- and posttranslocational ribosomes revealed by electron cryomicroscopy. *Cell*, **88**, 19–28.

Stark,H., Rodnina,M., Rinkeappel,J., Brimacombe,R., Wintermeyer,W. and van Heel,M. (1997b) Visualisation of elongation factor Tu on the *Escherichia coli* ribosome. *Nature*, **389**, 403–406.

Triman,K., Becker,E., Dammel,C., Katz,J., Mori,H., Douthwaite,S., Yapijakis,C., Yoast,S. and Noller,H.F. (1989) Isolation of temperature-sensitive mutant of 16S rRNA in *Escherichia coli*. *J. Mol. Biol.*, **209**, 645–653.

Verschoor,A., Frank,J., Radermacher,M., Wagenknecht,T. and Boublik,M. (1984) Three-dimensional reconstruction of the 30 S ribosomal subunit from randomly oriented particles. *J. Mol. Biol*. **178**, 677–698.

Vila,A., Viril-Farley,J. and Tapprich,W.E. (1994) Pseudoknot in the central domain of small subunit ribosomal RNA is essential for translation. *Proc. Natl Acad. Sci. USA*, **91**, 11148–11152.

Wagenknecht,T., Grassucci,R. and Frank,J. (1988) Electron microscopy and computer image averaging of ice-embedded large ribosomal subunits from *Escherichia coli*. *J. Mol. Biol.*, **199**, 137–145

Wang,R., Alexander,R.W., VanLoock,M., Vladimirov,S., Bukhtiyarov,Y., Harvey,S. and Cooperman,B.S. (1999) Three-dimensional placement of the conserved 530 loop of 16S rRNA and its neighboring components in the 30S subunit. *J. Mol. Biol.*, **286**, 521–540.

Weller,J.W. and Hill,W.E. (1992) Probing dynamic changes in rRNA conformation in the 30S subunit of the *Escherichia coli* ribosome. *Biochemistry*, **31**, 2748–2757.

Wilson,K.S. and Noller,H.F. (1998) Molecular movement inside the translational engine. *Cell*, **92**, 337–349.

Received September 6, 1999;
revised and accepted September 21, 1999